

Simulating Collisional Dark Matter

Javier Alejandro Acevedo Barroso

September 24, 2018

Contents

1	Objectives	3
1.1	General Objective	3
1.2	Specific Objectives	3
2	Introduction	4
2.1	Dark Matter	4
2.1.1	The Cluster Missing Mass Problem	4
2.1.2	Galaxy Rotation Curves	5
2.2	Types of Dark Matter	6
2.3	The Boltzmann Equation	6
2.4	Lattice Automata and Lattice Boltzmann	6
2.5	BGK Approximation	6
3	The Lattice Boltzmann Algorithm	7
3.1	General Description	7
3.2	The Collisional Step	9
3.3	Units and Systems to Simulate	9
4	Results	10
4.1	No Collisional	10
4.2	Collisional with reported $\langle \sigma v \rangle$	10
4.3	Different Equilibrium Distributions	10
5	Conclusions	11
5.1	A Numerically Stable Simulation	11

Chapter 1

Objetives

1.1 General Objective

To simulate the phase space of a collisional dark matter fluid using a Lattice-Boltzmann Method

1.2 Specific Objectives

- To implement a Lattice-Boltzmann simulation using a 4-dimensional phase space and a varying collisional term.
- To implement a Lattice-Boltzmann simulation using a 6-dimensional phase space and a varying collisional term.
- To study the dynamical behavior of a dark matter fluid using different equilibrium distributions in the collisional term.
- To compare the phase space of a collisional dark matter fluid with its collisionless version.

Chapter 2

Introduction

In this work, we simulate the phase space of a collisional dark matter fluid. In order to follow the ideas and developments of the upcoming chapters, it is essential to understand some concepts and computational techniques. In this chapter, we present all the necessary knowledge for the proper understanding of this work.

2.1 Dark Matter

Modern cosmology describes the universe as being composed of two fundamental types of energy: dark energy and matter¹, with dark energy being associated with a cosmological constant and matter being divided into two categories: dark matter and standard model matter². The energy density of the universe is 69% dark energy and 31% matter.

Standard model matter includes all the particles whose interactions can be properly described by the standard model, such as: Protons, Electrons, Atoms and naturally, any structure that they form, like Humans or Stars. On the other hand, dark matter is all the matter we measure from astrophysical sources which cannot be explained by baryonic matter. We know of the existence of dark matter entirely from astrophysical evidence, during this section we are going to do an historical review of such evidence.

2.1.1 The Cluster Missing Mass Problem

The traditional history of dark matter begins in the 1930s with the swiss astronomer Fritz Zwicky[1] [2], who noticed an unusually high velocity dispersion between the galaxies of the Coma Cluster. To tackle the problem, Zwicky assumed that the Coma Cluster “had already reached a mechanically stationary state” [3] and such, the virial theorem could be applied. By counting galaxies, along with assuming that matter is distributed uniformly in the cluster and using Hubble’s estimate of the mean mass of a galaxy, Zwicky was able to estimate the potential energy of the Cluster. Using his estimate of the visible mass and the virial theorem, Zwicky concluded that the velocity dispersion must be $\sqrt{v^2} = 80$ km/s. Nonetheless, the real measurement of the velocity dispersion

¹In relativity, mass and energy are equivalent.

²Which is very often called “Baryonic matter” due to Baryons being the largest fraction of this mass.

was $\sqrt{v^2} = 1000$ km/s, implying a virial mass about 400 times larger than the visible mass³. Zwicky called the discrepancy between the luminous matter (in the form of visible galaxies which could simply be counted) and the virial matter (obtained from the virial theorem and the high velocity dispersion of the cluster) “Dark Matter”.

By the late 1950s similar calculations for different clusters had been published. Many of those calculations had very large values for the mass-to-light ratio[4], which were consistent with the mass-to-light ratio calculated from the Coma Cluster. The problem of the missing mass seemed to appear in almost every large scale structure in the universe, and by the early 1970s astrophysicist had already disregarded hot gas[5] and free hydrogen[6] as explanations for the missing mass in Clusters. Nonetheless, it was still possible that the missing mass problem could be in fact solved by a more refined model of the cluster kinematics, because so far, the missing mass problem had only been observed on Clusters and large scale structures.

2.1.2 Galaxy Rotation Curves

A galaxy rotation curve plots the orbital velocity of stars in a galaxy versus their distance to the galaxy centre. These curves became important thanks to the work of the indian astrophysicist Subrahmanyan Chandrasekhar, who proved that the mutual interactions of stars were negligible, so a galaxy could be modeled as a non-interacting system of stars. Such modeling allows to obtain mass profiles from galaxy rotation curves. Now, due to photometric measurements, astrophysicist believed that most of the mass was overwhelmingly concentrated in the galaxy centre, therefore, it was reasonable to model the galaxy similarly to the solar system. Consider a star in the galaxy disk with mass m at a distance r from the galaxy centre, given that we can disregard the interaction between stars, the sum of forces acting on the object is simply the gravitational attraction towards the galaxy centre:

$$m \frac{v^2}{r} = G \frac{mM}{r^2} \quad (2.1)$$

With M being the mass enclosed by the star orbit and v being the orbital velocity of the star. Finally, the galaxy rotation curve for such galaxy will be given by:

$$v(r) = \sqrt{\frac{GM}{r}} \quad (2.2)$$

Which means that for objects outside of the galaxy disk (but still under the influence of the galaxy gravitational pull), the enclosed mass will be constant regardless of the radius, and thus, the orbital velocity will be proportional to $r^{-1/2}$. With the advent of radio astronomy and the invention of the Image Tube Spectrograph, astronomers were able to measure orbital velocities way beyond the apparent end of the luminous galaxy disks, only to find that the orbital velocity did not decay proportionally to $r^{-1/2}$ but it stayed more or less constant[7] [8] veraFirst. This behavior can be seen more easily in the figure 2.1

³This ratio is often called the mass-to-light ratio.

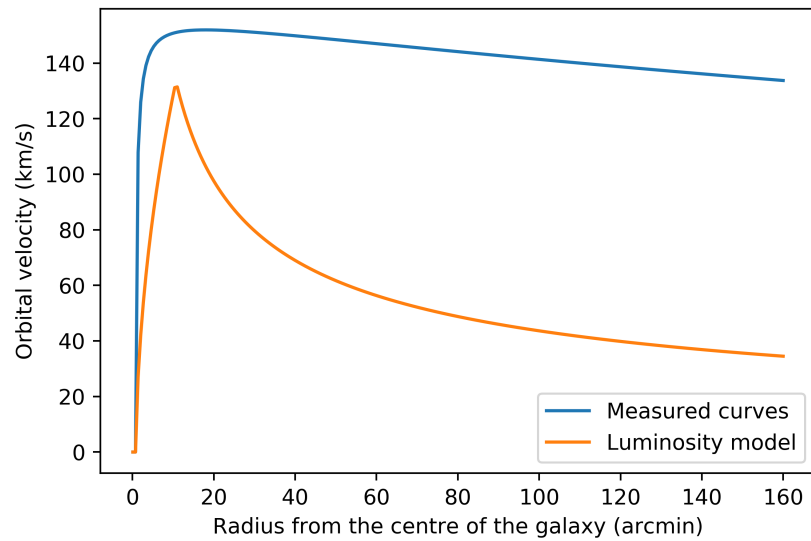


Figure 2.1: A comparison between the model from photometrical measurements and the curves measured. This curves are illustrative and do not correspond to a particular galaxy.

2.2 Types of Dark Matter

asd

2.3 The Boltzmann Equation

asdf

2.4 Lattice Automata and Lattice Boltzmann

asd

2.5 BGK Approximation

asd

Chapter 3

The Lattice Boltzmann Algorithm

3.1 General Description

As previously asserted, the heart of the Lattice-Boltzmann Algorithm lies on its discretization of the phase space[9] [10]. To discretize the phase space, one must first choose the region to simulate. In this work, we name the extremal values in the w axis of the phase space W_{min} and W_{max} . Then, one has to fix either the size of the grid or the size of the lattice. We named the size of the grid in the w axis N_w (i.e. N_x or N_{vz}). The size of the lattice in the w axis (dw) and the extremal values are related by:

$$dw = \frac{W_{max} - W_{min}}{N_w} \quad (3.1)$$

In this work we are going to use the density-velocity phase space. Now that we have properly defined the phase space grid, we can proceed to the initialization. For simplicity, we choose gaussian initial conditions given by:

$$f(\mathbf{r}, \mathbf{v}, 0) = A \exp \left\{ -\frac{\mathbf{r}^2}{\sigma_r^2} - \frac{\mathbf{v}^2}{\sigma_v^2} \right\} \quad (3.2)$$

Where $f(\mathbf{r}, \mathbf{v}, 0)$ is the initialization of the phase space, A is an indirect measure of the total mass in the system, \mathbf{r} is the vector $= (x, y, z)$, \mathbf{v} is the vector $= (vx, vy, vz)$, and σ_r and σ_v are a measure of the width of the gaussian profile in the given axis. After initialization, the system evolves by classical mechanics and the modelling of the collisional step, which can be seen more easily in figure [3.1](#)

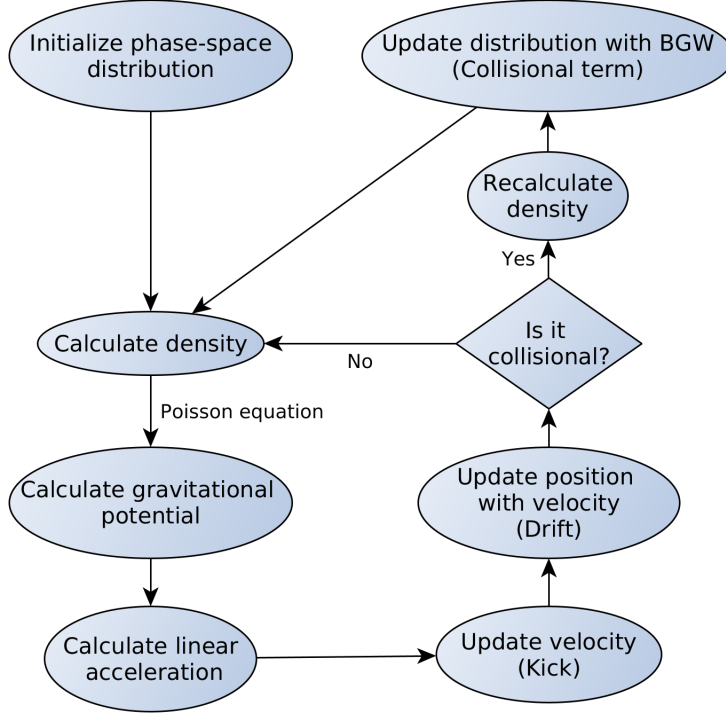


Figure 3.1: Flowchat of the algorithm.

Given the density-velocity phase space, the spatial density of matter is given by the integral:

$$\rho(\mathbf{r}, t) = \int_{-\infty}^{\infty} f(\mathbf{r}, \mathbf{v}, t) d\mathbf{v}.$$

Which, when evaluating in the lattice becomes:

$$\rho(\mathbf{r}, t) = \sum_{\mathbf{v}_{min}}^{\mathbf{v}_{max}} f(\mathbf{r}, \mathbf{v}, t) d\mathbf{v} \quad (3.3)$$

and during initialization:

$$\rho(\mathbf{r}, 0) = \sum_{\mathbf{v}_{min}}^{\mathbf{v}_{max}} f(\mathbf{r}, \mathbf{v}, 0) d\mathbf{v} \quad (3.4)$$

Once we have calculated the density, we can use the Poisson equation to calculate the potential due the gravitational force[10]

$$\nabla^2 \Phi(\mathbf{r}, t) = 4\pi G \rho(\mathbf{r}, t) \quad (3.5)$$

To solve the Poisson equation we use the pseudo-spectral Fourier method, which allows for very fast numerical solutions by making use of the Fast Fourier Transform algorithm. The idea is simply

to apply a Fast Fourier Transform (FFT), then solve the equation in the Fourier space, and then apply an inverse transform (IFFT). In the phase space the Poisson equation is given by [11] [12]

$$\lambda_{\mathbf{k}}^2 \hat{\Phi}(\mathbf{k}, t) = 4\pi G \hat{\rho}(\mathbf{k}, t) \quad (3.6)$$

Where $\hat{g}(\mathbf{k}, t)$ is the Fourier transform of $g(\mathbf{r}, t)$, and $\lambda_{\mathbf{k}}$ is a constant that depends on the size of the lattice and the wavevector \mathbf{k} . $\lambda_{\mathbf{k}}$ is calculated according to the approximation scheme used to solve the equation, here we use the pseudo-spectral approximation, in which $\lambda_{\mathbf{k}}$ becomes:

$$\lambda_{\mathbf{k}}^2 = \left(\frac{2\pi k_x}{X_{max} - X_{min}} \right)^2 + \left(\frac{2\pi k_y}{Y_{max} - Y_{min}} \right)^2 + \left(\frac{2\pi k_z}{Z_{max} - Z_{min}} \right)^2 \quad (3.7)$$

Therefore, solving the Poisson equation is reduced to calculating $\hat{\Phi}(\mathbf{k})$ for every \mathbf{k} and then transforming out of Fourier space.

Once we have the potential, calculating the acceleration is straight-forward:

$$\mathbf{a}(\mathbf{r}, t) = -\nabla \Phi(\mathbf{r}, t) \quad (3.8)$$

Which, in the context of the lattice can be calculated simply with a central difference numerical derivative. Now, in order to update the phase space, we must first define the time interval to simulate: we name N_t the number of time intervals to simulate and dt the length of each of such intervals. After calculating the acceleration and defining dt , we can update our phase space, the subtlety here is that we will only use integer arithmetic, which means that we do not exactly care for the change in velocity during a time dt but for how many cells in the phase space that change represents. This is modeled by:

$$\mathbf{v}_{n+1} = \mathbf{v}_n + \lfloor \mathbf{a}_n dt \rfloor \quad (3.9)$$

With $\lfloor x \rfloor$ representing the operator “to nearest integer”, so that \mathbf{v} and $\lfloor \mathbf{a} dt \rfloor$ are vectors of integers and n represents the time instant. The update of the velocity is known as “kick”. Analogously, the update of the position is known as “drift”, and is given by:

$$\mathbf{r}_{n+1} = \mathbf{r}_n + \lfloor \mathbf{v}_n dt \rfloor \quad (3.10)$$

Using only integer arithmetics allows for the elimination of the rounding error but introduces lattice noise. Regardless, this method creates a one to one map with the continuous solution. [9] [10]

The “kick” and “drift” together are known as the “Streaming” step, and it represents the classical movement of particles under a potential but without considering the collision of particles. If we want a collisionless simulation, we can just calculate again the density and continue the algorithm from there. If we want a collisional simulation, we must define a collisional step.

3.2 The Collisional Step

As previously mentioned, solving the collisional integral is not straight-forward

3.3 Units and Systems to Simulate

Chapter 4

Results

4.1 No Collisional

4.2 Collisional with reported $\langle \sigma v \rangle$

4.3 Different Equilibrium Distributions

Chapter 5

Conclusions

5.1 A Numerically Stable Simulation

Bibliography

- [1] Gianfranco Bertone and Dan Hooper. A History of Dark Matter. *Submitted to: Rev. Mod. Phys.*, 2016.
- [2] J. M. Cline. TASI Lectures on Early Universe Cosmology: Inflation, Baryogenesis and Dark Matter. *ArXiv e-prints*, July 2018.
- [3] H. Andernach and F. Zwicky. English and Spanish Translation of Zwicky’s (1933) The Redshift of Extragalactic Nebulae. *ArXiv e-prints*, November 2017.
- [4] M. Schwarzschild. Mass distribution and mass-luminosity ratio in galaxies. 59:273, September 1954.
- [5] J. F. Meekins, G. Fritz, T. A. Chubb, and H. Friedman. Physical Sciences: X-rays from the Coma Cluster of Galaxies. 231:107–108, May 1971.
- [6] A. A. Penzias. Free Hydrogen in the Pegasus I Cluster of Galaxies. 66:293, March 1961.
- [7] D. H. Rogstad and G. S. Shostak. Gross Properties of Five Scd Galaxies as Determined from 21-CENTIMETER Observations. 176:315, September 1972.
- [8] M. S. Roberts and R. N. Whitehurst. The rotation curve and geometry of M31 at large galactocentric distances. 201:327–346, October 1975.
- [9] Sebastián Franco Ulloa. Simulaciones de un fluido débilmente auto-interactuante con métodos de lattice-boltzmann, 5 2017.
- [10] Philip Mocz and Sauro Succi. Integer lattice dynamics for Vlasov–Poisson. *Mon. Not. Roy. Astron. Soc.*, 465(3):3154–3162, 2017.
- [11] V. Fuka. PoisFFT - A Free Parallel Fast Poisson Solver. *ArXiv e-prints*, September 2014.
- [12] J.W Eastwood R.W Hockney. *Computer simulation using particles*.